SIMULATION ANALYSIS AND OPTIMIZATION OF SOIL CUTTING OF ROTARY BLADE BY ANSYS/LS-DYNA
/
基于 ANSYS/LS-Dyna 旋耕刀切土仿真分析及优化

Wusong XIAO [1], Po NIU [*1], Pan WANG [*2], Yingjie XIE [3], Fei XIA [4]
[1]College of Mechanical Engineering, Chongqing Three Gorges University, Chongqing/China;
[2]Sichuan Academy of Agricultural Machinery Science, Sichuan/China;
[3]Chongqing Agricultural Mechanization Technology Extension Station, Chongqing/China;
[4]Chongqing Kaizhou District Agriculture Service Center, Chongqing/China
Tel: +86 18883367182; E-mail: niupo205@163.com
Corresponding author: Po Niu, Pan Wang
DOI: https://doi.org/10.35633/inmateh-72-02

Keywords: *rotary blade, numerical simulation, SPH, optimization*

ABSTRACT
Mini-tiller is an indispensable agricultural machinery in hilly and mountainous areas of China. Rotary blade is an important working part of mini-tiller, which directly affects the operation quality and power consumption of mini-tiller. In order to reduce the cutting resistance and power consumption of the rotary blade of mini-tiller, the cutting process of the rotary blade was analyzed by numerical simulation, and the tangential bending radius (R), bending angle (β) and edge thickness (c) of the rotary blade were selected as factors to optimize it. After comparing the cutting resistance and cutting power consumption of the rotary blade before and after optimization, the results show that the cutting force of the optimized rotary blade is smaller than that of the rotary blade before optimization. The cutting power consumption of the optimized rotary blade is 2.4% lower than that of the unoptimized rotary blade, which achieves the purpose of drag reduction and consumption reduction.

摘要
微耕机是我国丘陵山区不可或缺的农业机械，旋耕弯刀是其重要的工作部件，直接影响其作业质量与功耗。为降低微耕机旋耕弯刀的切削阻力和功耗，本文通过数值模拟的方法对旋耕弯刀切土过程进行了分析，并选取旋耕弯刀的正切部弯折半径（R），弯折角（β），刃口厚度（c）作为因子对其进行了优化，优化前后旋耕弯刀的切削阻力和切土功耗的对比结果表明优化后的旋耕弯刀切削力小于优化前旋耕弯刀的切削力，旋耕弯刀切土功耗较优化前的旋耕弯刀切土功耗降低了2.4%，达到了减阻降耗的目的。

INTRODUCTION

Mini-tiller is an indispensable agricultural machinery in hilly and mountainous areas of China, which is mainly used for tillage and soil preparation in paddy fields and dry fields *(Niu et al.,2017)*. During the operation of the mini-tiller, the power is transmitted to the rotary blade through the conveying device. The rotary blade cuts the soil and completes the operations of cutting soil, crushing soil, and throwing soil (*Sun et al., 2022*). At the same time, the rotary blade is subjected to the reaction force of the soil and pushes the mini-tiller forward *(Li et al., 2016)*. Therefore, the cutting resistance of rotary tiller bend is not only related to the working quality of mini-tiller, but also the main influencing factor of mini-tiller power consumption. How to reduce the cutting resistance of rotary blade in the operation process of mini-tiller is the key link to improve the operation performance of mini-tiller and reduce the power consumption of mini-tiller.

At present, the research on rotary blade mainly focuses on the soil cutting process of rotary blade. Mootaz Abo-Elnor et al. simulated the interaction between rotary blades and soil using numerical simulation *(Mootaz et al., 2004)*. Jafar Habibi Asl selected three types of rotary blades, C-shaped, L-shaped and RC-shaped, for a comparative experiment on cutting power consumption by establishing a mathematical model of power consumption, revealing that the cutting power consumption of RC-type rotary blade was lower than that of the other two types *(Jafar., 2009)*.

Wusong Xiao, M.S. Stud. Eng.; Po Niu, Assoc. Prof. Ph.D. Eng.; Pan Wang, Senior engineer. M.S. Eng.; Yingjie Xie, Senior engineer. M.S. Eng.; Fei Xia, Senior engineer. M.S. Eng.

Alavi and Hojati numerically simulated the process of rotary blades cutting soil using the finite element method, and the results showed that increasing the forward speed of the machinery would reduce soil stress, while increasing the rotary speed of rotary blades and soil moisture content would increase soil stress *(Alavi et al., 2012).* To optimize the geometry of rotary blades, Matin M.A. et al. studied the torque, power consumption, and energy characteristics of three types of blades (conventional, half-width and straight) at four rotary speeds (125, 250, 375 and 500 rpm). Through testing, the average and maximum power of all blades increased with the increase in rotary speed. At a rotary speed of 500 r/min, the power consumption of straight blade was 25% lower than that of conventional blade *(Matin M.A., 2015)*; Subrata Kumar Mandal et al. optimized the energy consumption of L-shaped rotary blade by establishing a mathematical model *(Subrata et al., 2016)*. Li Shoutai and Li Yunwu used SPH method to simulate the soil cutting process of rotary blade *(Li et al.,2018; Li et al., 2019)*; Zhu Liuxian and Sun Yong et al. used the finite element method to analyze the soil cutting process of rotary blade roller *(Zhu., 2020)*; Nelson Richard Makange et al. studied the mechanical properties between rotary blades and soil at different rotary speeds and tillage depths using the discrete element method (DEM) *(Nelson et al., 2020)*. Yeon-Soo Kim et al. predicted and analyzed the cutting force of rotary blades with tillage depth as a function, and analyzed the impact of different tillage depths on soil properties based on DEM, providing a theoretical basis for the design of agricultural machinery *(Yeon-Soo et al., 2021)*. Zhu et al. conducted an optimization analysis using DEM on the performance of rotary blades for cutting soil and crushing stubble *(Zhu et al., 2022)*. However, most studies have focused on the interaction between the soil and the rotary blade, while there has been relatively little research on the optimization of the structure and cutting power consumption of the rotary blade. The structure and geometric parameters of rotary blade directly affect the power consumption of soil cutting. A reasonable structure of rotary blade can reduce the cutting resistance and reduce the cutting power consumption *(Du et al., 2020)*. Therefore, this paper selects the rotary blade of the mini-tiller as the research object, and analyzes the soil cutting process of the rotary blade by numerical simulation. The tangent bending radius (R), bending angle (β) and blade thickness (c) of the rotary blade are selected as the test factors to optimize the rotary blade. Through the analysis of the numerical simulation results before and after, the optimal combination of the lowest power consumption of the rotary blade in the soil cutting process is obtained. This provides a theoretical basis and reference for the optimization of rotary blade and the performance improvement of mini-tiller.

MATERIALS AND METHODS

The main structure and parameter name of rotary blade

The structure of rotary blade is mainly composed of side cutting edge, positive cutting edge, handle and installation hole. The structure is shown in Fig.1. *(Md.A.Matin et al., 2021)*.

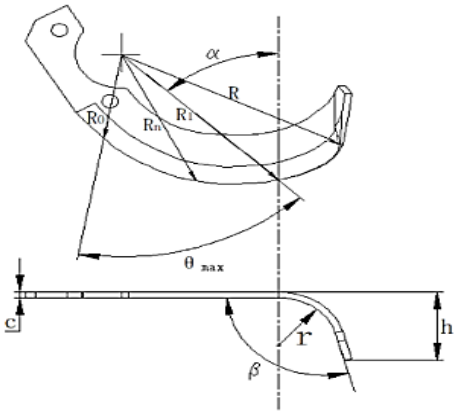

Fig. 1 – Rotary blade construction

R-rotation radius, R_0-initial radius of side-cutting edge, R_1-terminal radius of side-cutting edge, R_n-radius of any point of side-cutting edge, α - angle between end radius of side-cutting edge and bending line, θ_{max}-wrap angle of side-cutting edge, β-bending angle, r - bending radius, h-working width

Motion analysis of rotary blade

In the operation process of the mini-tiller, on the one hand, the rotary blade rotates around the cutter shaft, and on the other hand, it moves forward with the machine. Therefore, the absolute motion of the rotary blade is the vector sum of its rotary motion and forward motion, and the motion trajectory is a trochoid *(Fang et al., 2020)*.

Taking the knife roller rotation center as the coordinate origin, the forward direction of the rotary tiller is the positive direction of the x-axis, and the y-axis is positive downward. The coordinate system shown in Fig. 2 is established *(Zhang et al., 2022)*.

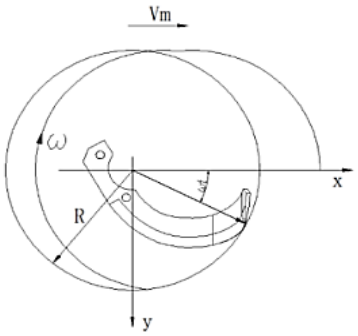

Fig. 2 – Trajectory diagram of rotary blade

If the forward speed of the micro tillage machine is v_m, the angular velocity of the rotary blade is ω. The motion equation is as follow *(Abdullah Al Musabbir et al., 2022):*

$$x = R\cos\omega t + v_m t \tag{1}$$

$$y = R\sin\omega t \tag{2}$$

R - rotary radius of blade roller [mm];
ω - rotational angular velocity of rotary blade [rad/s];
v_m - forward speed of Mini-tiller [m/s];
t - time [s].

From the formulas (1) and (2), it can be seen that the x coordinate and y coordinate corresponding to the end point of the rotary tiller bender in the rectangular coordinate system change with time, and the time there is the independent variable *(Matin MA et al., 2014)*. Therefore, the speed of the tool on the x axis and the speed on the y axis can be obtained only by deriving the formulas (1) and (2) respectively:

$$v_x = \frac{dx}{dt} = v_m - R\omega\sin\omega t \tag{3}$$

$$v_y = \frac{dy}{dt} = R\omega\cos\omega t \tag{4}$$

v_x-velocity component in x-axis direction
v_y-velocity component in y-axis direction

According to the formula (3) and formula (4), the absolute speed of the rotary blade at work can be obtained:

$$v = \sqrt{v_x^2 + v_y^2} = \sqrt{v_m^2 + R^2\omega - 2v_m\omega\sin\omega t} \tag{5}$$

v - absolute speed of rotary blade in the working process [m/s]

Linear velocity formula of the end point of the rotary blade is:

$$v_p = R\omega \tag{6}$$

v_p - linear velocity of the end point of the rotary blade

Rotary tillage speed ratio λ is

$$\lambda = \frac{v_p}{v_m} = \frac{R\omega}{v_m} \tag{7}$$

$$v_x = v_m - R\omega\sin\omega t = v_m(1 - \lambda\sin\omega t) \tag{8}$$

When the rotary blade cuts the soil backwards, it is necessary to make $v_x < 0$. From the formulas (7) and (8), it can be seen that $\lambda > 1$. Therefore, the circular line speed of the end point of the rotary blade is greater than the forward speed of the rotary tiller. The cutting trajectory of the rotary blade is shown in Fig. 2.

Finite element model of rotary blade

The rotary blade model established in UG 10.0 is saved in *CATPart or *IGES format and imported into ANSYS/Ls-dyna. The unit type of rotary blade is set to “Thin shell 163”, and the unit is defined as a constant *(Tagar et al., 2015)*. The material of the tool is set to be a rigid body type material, the density is defined as 7800 kg/m^3, the Young's modulus is defined as 207 GPa, and the Poisson's ratio is defined as 0.35 *(Ma et al., 2022)*. The unit size of the grid is set to 1 mm, and the free grid is divided and checked and optimized. The number of units is 25274, and the number of unit nodes is 25254. The finite element model of the rotary blade is shown in Fig. 3 *(Li et al., 2019)*. The finite element model of the rotary blade is saved in the form of *k* files.

Fig. 3 – Finite element model of rotary blade

Establishment of finite element model of soil

By consulting the literature, the common cultivated soil in hilly and mountainous areas was selected as the basis for soil parameter setting, as shown in table 1 *(Manuwa, 2009; A.A. Tagar et al., 2014)*. The finite element model of the rotary blade is imported into Ls-Prepost, and the SPH soil model is established according to the global coordinate system of the rotary blade *(Zeng et al., 2021; Lu et al., 2014)*. The soil material is MAT147 material model *(Bahrami et al., 2020)*, the length of the soil is 400 mm, the width is 300 mm, and the height is 200 mm. The soil model is shown in Fig. 4 *(Zhang et al., 2019)*.

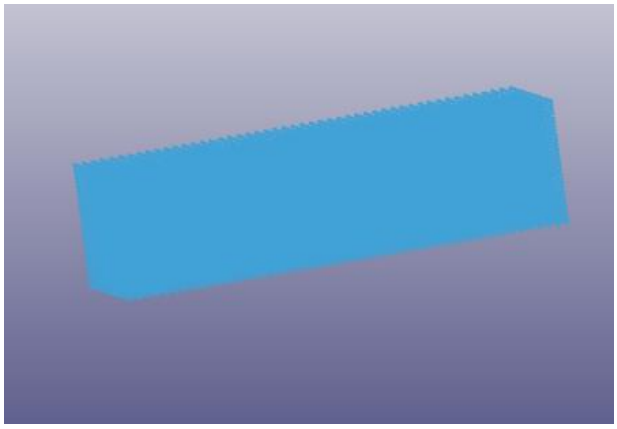

Fig. 4 – SPH Model of Soil

Table 1

Soil parameters

Parameter name	Soil density [kg/m^3]	Bulk modulus [Pa]	Specific gravity of soil particle	Water content [%]	Shear modulus [Pa]	Internal friction angle [radian]
Value selection	2350	3.5e+7	2.68	21	2.0e+7	0.436

Setting of boundary conditions

According to the actual situation of soil cutting by rotary blade, the degree of freedom of movement of the bottom and both sides of the soil model in the x, y and z directions is constrained. The rotary blade rotates around the cutter shaft and moves forward with the unit.

Therefore, the degree of freedom of rotation and movement of the rotary blade in the y-axis direction, the degree of freedom of rotation in the x-axis direction and the degree of freedom of movement in the z-axis direction are constrained. AUTOMATIC_NODES_TO_SUFACE is used to set the contact between the rotary blade and the soil to ensure that the surface unit of the soil can be automatically defined by the program even in the case of cutting failure *(Li et al., 2018)*.

The forward speed of the rotary blade is set to 0.25 m/s, the rotation angular velocity is set to 0.022 rad/s, the calculation time step is set to 0.1 ms, and the forced termination time is set to 300 ms *(Viktor et al., 2018)*.

Parameter optimization of rotary blade

Through the numerical simulation analysis process analysis and related data, the tangent bending radius (R), bending angle (β), and edge thickness (C) were selected as the test factors for optimizing the rotary blade.

Quadratic regression orthogonal design

(1) Determine the number of tests

Number of combined design trials

$$N = m_c + 2p + m_0 \tag{9}$$

In the formula, m_c is the number of comprehensive test points with two levels of each factor; p is the number of test factors; m_0 is the number of repeated tests with zero level for each factor.

Three factors were selected in this experiment, that is, $p = 3$, $m_c = 8$, and three groups were arranged at the zero level, that is, $m_0 = 3$, so the total number of tests can be obtained as $N = 17$. According to the r^2 value table, $r^2 = 1.831$, that is, the asterisk arm $r = 1.353$.

(2) Coding of factor level

The range of bending radius (R) is 30 mm -50 mm and the range of bending angle (β) is $90\text{-}120^{o}$. The value range of edge thickness (C) is 0.5 mm-1.5 mm.

The coding formula of horizontal factor is:

$$\begin{cases} z_{0j} = \dfrac{z_{1j} + z_{2j}}{2} \\ \Delta j = \dfrac{z_{2j} - z_{0j}}{r} = \dfrac{z_{2j} - z_{1j}}{2r} \\ x_j = \dfrac{z_j - z_{0j}}{\Delta j} \end{cases} \tag{10}$$

In the formula, z_{2j} and z_{1j} are the upper and lower limits of factor z_j respectively, and Δj is the change interval of factor z_j. According to formula (10), the three factors are coded, and the coding of the factor levels is shown in Table 2.

Table 2

Coding table of factor levels

x_j	z_j	R [mm]	β [º]	C [mm]
r	z_{2j}	50	120	1.5
1	$z_{0j} + \Delta j$	47.39	116.09	1.37
0	z_{0j}	40	105	1
-1	$z_{0j} - \Delta j$	32.61	93.91	0.63
-r	z_{1j}	30	90	0.5
Δj	$z_{2j} - z_{0j}/r$	7.39	11.09	0.37
Coding formula	$z_j - z_{0j}/\Delta j$	$x_1 = R - 40/7.39$	$x_2 = \beta - 105/11.09$	$x_2 = C - 1/0.37$

(3) Preparation of test plan

The quadratic orthogonal combination test plan and the corresponding rotary blade cutting simulation power are shown in Table 3.

Table 3

Analysis table of test plan

Test number	x_0	x_1	x_2	x_3	p [kW]
1	1	1	1	1	0.4980
2	1	1	1	-1	0.6053
3	1	1	-1	1	0.6112
4	1	1	-1	-1	0.6367
5	1	-1	1	1	0.4986
6	1	-1	1	-1	0.5642
7	1	-1	-1	1	0.5150
8	1	-1	-1	-1	0.5213
9	1	1.353	0	0	0.5782
10	1	-1.353	0	0	0.5712
11	1	0	1.353	0	0.5412
12	1	0	-1.353	0	0.6435
13	1	0	0	1.353	0.5086
14	1	0	0	-1.353	0.5420
15	1	0	0	0	0.5980
16	1	0	0	0	0.6160
17	1	0	0	0	0.6200

(4) The test scheme analysis table is imported into excel, and the interaction terms and centralization of factors x_1, x_2 and x_3 are compiled. The coefficients, variances and analysis results of the regression equation are calculated as shown in Table 4.

Table 4

Analysis results

Variation source	B_j	a_j	b_j	SS_j	F_j	α_j
x_0	9.687	17	0.567			
x_1	0.263	11.661	0.0225	5.912e-3	9.271	0.01 ~ 0.05
x_2	-0.270	11.661	-0.0231	6.266e-3	9.826	0.01 ~ 0.05
x_3	-0.263	11.661	-0.0226	5.963e-3	9.351	0.01 ~ 0.05
x_1x_2	-0.170	8	-0.0212	3.617e-3	5.672	0.01 ~ 0.05
x_1x_3	-0.060	8	-0.0075	4.490e-4	0.704	>0.25
x_2x_3	-0.155	8	-0.0193	2.999e-3	4.703	0.25
x_1'	-0.071	6.703	-0.0106	7.540e-4	1.182	>0.25
x_2'	-0.006	6.703	-0.0009	6.260e-6	9.82e-3	>0.25
x_3'	-0.251	6.703	-0.0375	9.471e-3	14.852	0.01

It can be seen from Table 5 that the values of α_{13}, α_1' and α_2' are greater than 0.25, indicating that the significance level of regression coefficients of x_1x_3, x_1' and x_2' are not significant, and should be removed from the regression equation.

The values of α_1,α_2,α_3 and α_{12} are all between 0.01 and 0.05, the value of α_{23} is less than 0.25, and the value of α_3' is less than 0.01, indicating that the significance level of regression coefficients of x_1, x_2, x_3, x_1x_2, x_2x_3, x_3' is significant, and the significance level of regression coefficients of x_3' is very significant, which should be retained in the regression equation.

Therefore, the regression equation is:

$$P = 0.5927 + 0.0225x_1 - 0.0231x_2 - 0.0226x_3 - 0.0212x_1x_2 - 0.0193x_2x_3 - 0.0375x_3^2 \quad (11)$$

(5) Calculation of sum of squares and F test

The total deviation sum of squares and the degree of freedom are:

$$ss_{total} = \sum_{i=1}^{N} p_i^2 - \frac{1}{N}\left(\sum_{i=1}^{N} P_i\right)^2 = \sum_{i=1}^{17} p_i^2 - \frac{1}{17}\left(\sum_{i=1}^{17} p_i\right)^2 = 0.0399 \quad (12)$$

$$df_{total} = N - 1 = 16 \quad (13)$$

The regression equation consists of six variables. Regression sum of square and regression degree of freedom are:

$$ss_{regression} = \sum_{i=1}^{6} ss_j = 0.034228 \quad (14)$$

$$df_{regression} = 6 \quad (15)$$

The sum of error squares and the degree of freedom of error are:

$$ss_e = \sum_{i=1}^{3} (p_{0i} - 0.6058) = 1.7E-4 \quad (16)$$

$$df_e = m - 1 = 2 \quad (17)$$

Residual sum of square and degree of freedom are:

$$ss_{residual} = ss_{total} - ss_{regression} = 5.673E-3 \quad (18)$$

$$df_{residual} = df_{total} - df_{regression} = 10 \quad (19)$$

Lack of fit sum of squares and degrees of freedom are

$$ss_{Lf} = ss_{residual} - ss_e = 5.503E-3 \quad (20)$$

$$df_{Lf} = df_{residual} - df_e = 8 \quad (21)$$

Regression equation test:

$$F_{regression} = \frac{ss_{regression}/df_{regression}}{ss_{residual}/df_{residual}} = 10.056 > F_{0.01}(6,10) = 5.385 \quad (22)$$

Lack of fit test:

$$F_{Lf} = \frac{ss_{Lf}/df_{Lf}}{ss_e/df_e} = 8.0926 < F_{0.1}(8,2) = 9.3667 \quad (23)$$

After regression equation test and lack of fit test, the significance level of regression equation (11) is $\alpha = 0.01$, that is, the regression of regression equation is particularly significant.

Parameter optimization of rotary blade

The objective function (11) is established with the goal of minimizing the power consumption of rotary blade. The constraint condition is:

$$\begin{cases} x_1 \in [-1.353, 1.353] \\ x_2 \in [-1.353, 1.353] \\ x_3 \in [-1.353, 1.353] \end{cases} \quad (24)$$

According to the optimized objective function and constraint conditions, the optimal solution of the minimum value of the objective function is x_1=0.96, $x_2 = -0.48$, $x_3 = 0.0468$, that is, R=47.09 mm, $\beta = 99.8^\circ$, $c = 1.017\text{mm}$. The theoretical power consumption of soil cutting is 0.4921 kW. According to the optimized parameters of the rotary blade, the rotary blade model is optimized, and the soil cutting dynamics simulation of the optimized rotary blade is carried out.

RESULTS

In the process of cutting soil, the side cutting edge of the rotary blade which is close to the soil first cuts the soil along the longitudinal direction to realize the function of cutting soil. Under the extrusion of the rotary blade, the soil begins to undergo plastic deformation. As the rotary blade rotates around the cutter shaft, the tillage depth of the rotary blade gradually deepens, and the tangent edge and the tangent part begin to contact the soil. The rotary blade cuts the soil horizontally. The contact area between the rotary blade and the soil continues to increase, and the shear and extrusion of the soil continue to increase. The soil unit is invalidated and deleted and broken along the blade surface. Under the combined action of the side cutting edge, the side cutting edge, the side cutting part, the tangent part and the back of the rotary blade, the soil is squeezed and deformed and finally broken and flipped, so as to achieve the effect of breaking soil, breaking soil, throwing soil and weeding by the rotary blade. The simulation results of the rotary blade cutting soil at a certain time are shown in Fig.5.

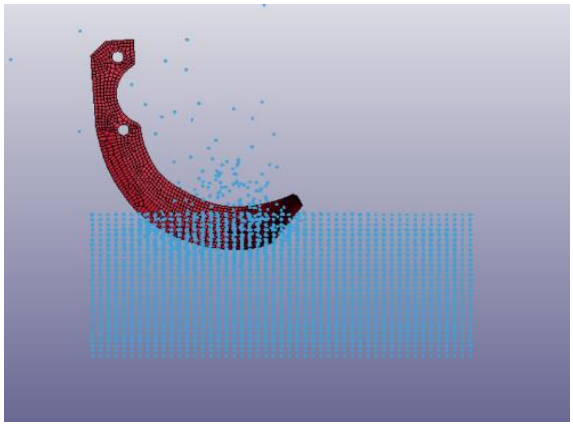

Fig. 5 – Simulation results of rotary blade cutting soil at a certain moment

The time history curve of the cutting force of the rotary blade before and after optimization is shown in Figs. 6(a) and 6(b). According to the time history curve of the cutting force, in a rotation cycle, the rotary blade begins to cut the soil, and the soil is squeezed by the rotary blade. The elastic deformation occurs, and the cutting force increases with the increase of the tillage depth of the rotary blade. When the tillage depth of the rotary blade is the largest, the cutting resistance reaches the maximum value of 1.04 kN. The rotary blade continues to do rotary motion, and the cutting force decreases with the decrease of tillage depth. When the soil is cut, the cutting force becomes 0 kN when the rotary blade leaves the soil, which is consistent with the force of the rotary blade in the actual operation. By comparing the time history curves of the cutting force of the rotary blade before and after optimization, it can be seen that the cutting force of the optimized rotary blade is smaller than that of the rotary blade before optimization, indicating that the optimization of the rotary blade has played a role in reducing the cutting force of the rotary blade.

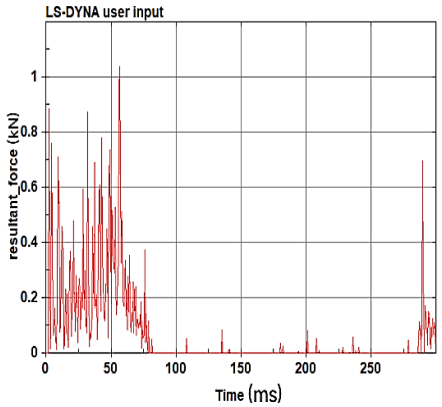

Fig.6(a) – Time history curve of cutting force before optimization

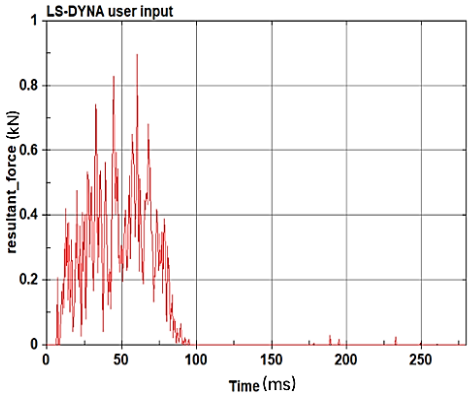

Fig. 6(b) – Time history curve of cutting force after optimization

In the LS-PrePost (post-processing software), the time-history curves of the total energy of the rotary blade before and after optimization are shown in figs. 7(a) and 7(b). It can be seen that when the rotary blade starts to cut the soil, the cutting energy increases. With the rotation of the rotary blade, the tillage depth continues to deepen, the area of contact between the rotary blade and the soil continues to increase, and the energy consumed by the soil is also increasing.

The total energy reaches the maximum value of 295J after the rotary blade completed one cutting of the soil, and tends to be stable, which is consistent with the actual working conditions. The soil cutting energy data of the rotary blade before and after optimization are imported into Excel respectively. The soil cutting power consumption of the rotary blade before optimization is 0.507 kW, and the soil cutting power consumption of the optimized rotary blade is 0.495 kW. Through comparative calculation, the soil cutting power consumption of the optimized rotary blade is 2.4% lower than that before optimization, which achieves the purpose of optimization.

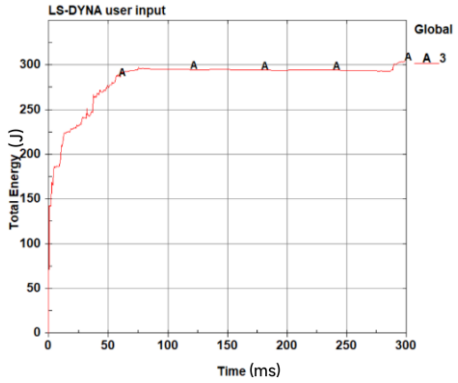

Fig. 7(a) – Energy time history diagram before optimization

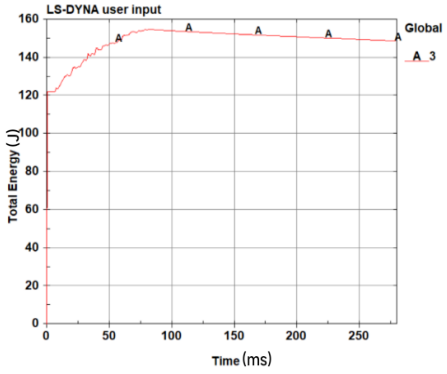

Fig. 7(b) – Energy time history diagram after optimization

CONCLUSIONS

(1) From the cutting force curve of the rotary blade before optimization, it can be seen that the cutting force increases with the increase of the tillage depth of the rotary blade. When the tillage depth of the rotary blade is the largest, the cutting resistance reaches the maximum value of 1.04 kN. The rotary blade continues to do rotary motion, and the cutting force decreases with the decrease of tillage depth. When the soil cutting is completed, the rotary blade leaves the soil and the cutting force becomes 0 kN, which is consistent with the force of the rotary blade in the actual operation.

(2) From the cutting power consumption curve of the rotary blade before optimization, it can be seen that the cutting power consumption of the rotary blade increases with the increase of the tillage depth of the rotary blade. When the cutting is completed, the rotary blade leaves the soil, and the cutting power consumption reaches the maximum value of 295 J and tends to be stable, which is consistent with the actual working conditions.

(3) Through the orthogonal test, the geometric parameters of the rotary blade were optimized. The cutting force rate of the optimized rotary blade was lower than that of the rotary blade before optimization, and the energy consumption of cutting soil was reduced by 2.4% compared with that before optimization. This provides a theoretical basis and reference for the improvement of the comprehensive performance of the micro-tiller and the optimization of the rotary tiller.

ACKNOWLEDGEMENT

The work was supported by the Chongqing Municipal Education Commission (KJQN202101207),and the Chongqing Wanzhou District Science and Technology Bureau (202206051958331768), and the Start-up fee for scientific research of high-level talents in Chongqing Three Gorges University (2014/0903341).

REFERENCES

[1] Abdullah Al Musabbir., Md Abedur Rahman., et al. (2022) Performance Evaluation of New Rotary Blades and Roller Cutter of Versatile Multi-Crop Planter on Residue Management, *Sarhad Journal of Agriculture*, 38(05):211-221. https://doi.org/10.17582/journal.sja/2022/38.5.211.221

[2] Alavi N. and Hojati R. (2012) Modeling the soil cutting process in rotary tillers using finite element method. Journal of Agricultural Technology 8(1): 27-37. https://doi.org/10.1016/j.jclepro.2011.05.006

[3] Chengcheng Ma., Shujuan Yi.,et al. (2022) A rotary blade design for paddy fields with long rice straw based on EDEM, *Engenharia Agrícola*, 43(03):62-72, https://doi.org/10.1590/1809-4430

[4] Du F., Liu J. (2020). Optimal combination and soil cutting analysis of rotary tillage knife in micro tiller based on orthogonal optimization (基于正交优化的微耕机旋耕刀优化组合及切土分析). *Ningxia Engineering Technology*, 19(04): 302-307+313. https://doi.org/10.3969/j.issn.1671-7244.2020.04.004

[5] Gongshuo Zhang, Zhiqing Zhang, et al. (2019) Soil-cutting simulation and parameter optimization of rotary blade's three-axis resistances by response surface method, *Computers and Electronics in Agriculture*, 164:104902. https://doi.org/10.1016/j.compag.2019.104902

[6] Hao Zhu.,Xiaoning He., et al. (2022) Evaluation of Soil-Cutting and Plant-Crushing Performance of Rotary Blades with Double-Eccentric Circular-Edge Curve for Harvesting Cyperus esculentus, *Advances in Agricultural Engineering Technologies and Application*, 12(06):862. https://doi.org/10.3390/agriculture12060862

[7] Huimin Fang.,Qingyi Zhang., Farman Ali Chandio.,et al. (2016) Effect of straw length and rotavator kinematic parameter on soil and straw movement by a rotary blade. *Engineering in Agriculture, Environment and Food*, 09(03):235-241, https://doi.org/10.1016/j.eaef.2016.01.001

[8] Jafar Habibi Asl., Surendra Singh. (2009). Optimization and evaluation of rotary tiller blades: Computer solution of mathematical relations. *Soil & Tillage Research*, 106(1):1-7. https://doi.org/10.1016/j.still.2009.09.011

[9] Jiang T., Zhang X., et al. (2009). 3D Numerical Simulation and Optimization of Soil Cutting Tools Based on SPH Method (基于 SPH 法的土壤切削刀具三维数值模拟及优化). *Electromechanical Engineering*, 26(6): 44-46. https://doi.org/10.3969/j.issn.1001-4551.2009.06.013

[10] Li S., Chen X., Chen W., et al. (2018). Soil-cutting simulation and parameter optimization of handheld tiller's rotary blade by Smoothed Particle Hydrodynamics modelling and Taguchi method. *Journal of cleaner production*, 179:55-62. https://doi.org/10.1016/j.jclepro.2017.12.228

[11] Li Y., Zhang G., et al. (2019). Development of sectional spiral rotary tillage cutter for low-power small vertical shaft deep plow (低功耗小型立轴式深耕机分段螺旋旋耕刀具的研制). *Journal of Agricultural Engineering*, 35(4):80-88. https://doi.org/10.11975/j.issn.1002-6819.2019.04.009

[12] Lu C., He J., et al. (2014). Simulation of soil cutting process of plane cutter based on SPH algorithm (基于 SPH 算法的平面刀土壤切削过程模拟). *Journal of Agricultural Machinery*, (8):134-139. https://doi.org/10.6041/j.issn.1000-1298.2014.08.022

[13] Manuwa S.I. (2009). Performance evaluation of tillage tines operation under different depths in a sandy clay loam soil. *Soil & Tillage Research*, 103(2): 399-402. https://doi.org/10.1016/j.still.2008.12.004

[14] Matin M.A., Fielke J.M., Desbiolles J.M.A. (2015). Torque and energy characteristics for strip-tillage cultivation when cutting furrows using three designs of rotary blade. *Biosystems Engineering*, 129(1): 329–340. https://doi.org/10.1016/j.biosystemseng.2014.11.008

[15] Matin M.A., Fielke J.M., Desbiolles J. (2014) Furrow parameters in rotary strip-tillage: effect of blade geometry and rotary speed. *Biosystems Engineering*, 118: 7-15. https://doi.org/10.1016/j.biosystemseng.2013.10.015

[16] Md. A. Matin., Md. I. Hossain., et al. (2021) Optimal design and setting of rotary strip-tiller blades to intensify dry season cropping in Asian wet clay soil conditions, *Soil and Tillage Research*, 02(07):235-245. https://doi.org/10.1016/j.still.2020.104854

[17] Milkevych Viktor, Munkholm J. Lars, et al. (2018) Modelling approach for soil displacement in tillage using discrete element method, *Soil & Tillage Research*, 183:60-71. https://doi.org/10.1016/j.still.2018.05.017

[18] Mootaz Abo-Elnor., R Hamilton., et al. (2004). Simulation of soil–blade interaction for sandy soil using advanced 3D finite element analysis. *Soil & Tillage Research*, 75(1): 61–73. https://doi.org/10.1016/s0167-1987(03)00156-9

[19] Mostafa Bahrami, Mojtaba Naderi-Boldaji, et al. (2020) Simulation of plate sinkage in soil using discrete element modelling: Calibration of model parameters and experimental validation, *Soil & Tillage Research*, 203:104700. https://doi.org/10.1016/j.still.2020.104700

[20] Nelson Richard Makange, Changying Ji, et al. (2020) Prediction of cutting forces and soil behavior with discrete element simulation, *Computers and Electronics in Agriculture*, 179,5848. https://doi.org/10.1016/j.compag.2020.105848

[21] Niu P., Yang M.J., Chen J., et al. Structural optimization of handrail of a handheld tiller by vibration modal analysis, *INMATEH-Agricultural Engineering*, 2017, 52(2): 91-98.

[22] Li S.T., Yang L., Niu P., et al. Design and study on the edge curve of blade of a handheld tiller's rotary blade, *INMATEH-Agricultural Engineering*, 2016, 51(3): 5-12.

[23] Shoutai Li, Xiaobing Chen, et al. (2018) Soil-cutting simulation and parameter optimization of handheld tiller's rotary blade by Smoothed Particle Hydrodynamics modelling and Taguchi method, *Journal of*

Cleaner Production, 179:55-62. https://doi.org/10.1016/j.jclepro.2017.12.228

[24] Subrata Kumar Mandalt., Basudeb Bhattacharyya‡., et al. (2016). Design Optimization of Rotary Tiller Blade using Specific Energy Requirement. *International Journal of Current Engineering and Technology*, 6(04),1257-1263. https://doi.org/10.14741/Ijcet/22774106/6.4.2015.31

[25] Sun Y., Zhu L., et al. (2022). Design and Simulation Analysis of the Mini-Tiller Rotary Blade Roller (微耕机旋耕刀辊的设计与仿真分析). *Mechanical Research & Application*, 35(03):34-36+42. https://doi.org/10.16576/j.ISSN.1007-4414.2022.03.010

[26] Tagar A.A., Changying Ji et al. (2014) Soil failure patterns and draft as influenced by consistency limits: An evaluation of the remolded soil cutting test, *Soil & Tillage Research*, 137:58-66. https://doi.org/10.1016/j.still.2013.12.001

[27] Tagar A A, Ji C Y, Jan A, Julien M, Chen S Q, Ding Q S, et al. (2015) Finite element simulation of soil failure patterns under soil bin and field testing conditions. *Soil & Tillage Research*, 145: 157–170. https://doi.org/10.1016/j.still.2014.09.006

[28] Xiao M., Buttons, et al. (2022). Design and analysis of torsion reduction and consumption reduction performance of self-excited vibration rotary tillage knife (自激振动旋耕刀设计与减扭降耗性能分析). *Transactions of the Chinese Society for Agricultural Machinery*, 53(11):52-63. https://doi.org/10.6041/j.issn.1000-1298.2022.11.006

[29] Xiongye Zhang, Lixin Zhang, Xue Hu, et al. (2022) Simulation of Soil Cutting and Power Consumption Optimization of a Typical Rotary Tillage Soil Blade. *Applications of Computer Science in Agricultural Engineering*. 12(16):8177, https://doi.org/10.3390/app12168177

[30] Yanshan Yang, John Fielke, et al. (2018) Field experimental study on optimal design of the rotary strip-till tools applied in rice-wheat rotation cropping system, *International Journal of Agricultural and Biological Engineering*, 11(02):88-94. https://doi.org/10.25165/j.ijabe.20181102.3347

[31] Yeon-Soo Kim, Md. Abu Ayub Siddique, et al. (2021) DEM simulation for draft force prediction of moldboard plow according to the tillage depth in cohesive soil, *Computers and Electronics in Agriculture*, 189, 10638. https://doi.org/10.1016/j.compag.2021.106368

[32] Zeng Z., Ma X., et al. (2021). Application status and prospect of discrete element method in agricultural engineering research (离散元法在农业工程研究中的应用现状和展望). *Transactions of the Chinese Society for Agricultural Machinery,* 52(04):1-20. https://doi.org/10.6041/j.issn.1000-1298.2021.04.001

[33] Zhu L., Sun Y., et al. (2020). Simulation of Cutting Soil of the Mini-tiller Rotary Blade Roller Based on Finite Element Method (基于有限元法的微耕机旋耕刀辊切削土壤仿真). *Journal of Agricultural Mechanization Research*, 42(09), 8177. https://doi.org/10.13427/j.cnki.njyi.2020.09.007